JPhys Materials

PAPER • OPEN ACCESS

Advances in modelling electron energy loss spectra from first principles

Journal of Physics: Materials

OPEN ACCESS

RECEIVED
18 December 2020

REVISED
30 January 2021

ACCEPTED FOR PUBLICATION
3 March 2021

PUBLISHED
25 March 2021

PAPER

Advances in modelling electron energy loss spectra from first principles

Rebecca J Nicholls

Department of Materials, University of Oxford, Oxford OX1 3PH, United Kindom

E-mail: rebecca.nicholls@materials.ox.ac.uk

Keywords: EELS, simulation, first principles calculations, electron microscopy

Abstract

Electron energy loss (EEL) spectroscopy carried out within a (scanning) transmission electron microscope can provide chemical and bonding information with atomic resolution. The information that lies within the spectrum can be difficult to extract, and often reference spectra are used to identify atomic bonding environments. First principles simulations are able to relate features in spectra to atomistic models and are particularly important in the interpretation of spectra where there are no appropriate bulk references, such as those from nanomaterials or interfaces. This paper reviews the recent developments in first principles simulations of EEL spectra and highlights the potential for advances in our understanding of materials.

1. Introduction

When a beam of electrons passes through the sample in a (scanning) transmission electron microscope ((S)TEM), it can excite, amongst other things, phonons, plasmons or core-electrons within the material. Once the beam has interacted with the material, it can be dispersed to produce an electron energy loss, or EEL, spectrum. Different amounts of energy are required to excite phonons (up to hundreds of meV), plasmons (up to about 50 eV) and core-electrons (10–1000 s of eV), and so peaks corresponding to the different inelastic events appear in different parts of the EEL spectrum.

The approach taken to modelling an EEL spectrum depends on several factors: the part of the spectrum being studied (the phonon, plasmon or core-loss region), the material being studied, including if it is amorphous, molecular or crystalline (and the elements contained within it), and the specific edge being investigated. In an EEL experiment, we are probing the loss function [1], $L(q,\omega)$, which is related to the dielectric function, $\epsilon(q,\omega)$, by $L(q,\omega) = Im[-1/\epsilon(q,\omega)]$[1]. For modelling the plasmon region, the full dielectric function needs to be modelled, whilst when modelling the core-loss region it is possible to approximate the loss function by the imaginary part of the dielectric function [1]. Historically, rather than a full calculation of the EEL spectrum, core-loss edges have been interpreted using the local density of states, LDOS. This is still a common method for understanding the electronic properties of nano-materials. In addition, even in cases where the full spectrum is used to interpret experiment, LDOS can be an important tool for relating peaks in the spectrum to the structural model and electronic structure.

Several codes exist which can calculate EEL spectra from first principles including WIEN2k [7, 8], FEFF [9, 10], CASTEP [11, 12], Elk [13], Yambo [14, 15], ONETEP [16, 17] and MADNESS [18]. Different codes use different approximations and are suitable in different situations. An excellent description of the mechanics of modelling an EEL spectrum is given in Chapter 14 of Transmission Electron microscopy: Diffraction, Imaging, and Spectrometry [19] and readers are referred there (and to references within it) for more details about how to model EEL spectra.

[1] This response function is for the specific case of an infinite medium, and includes the macroscopic dielectric function. The macroscopic dielectric function was related to the microscopic dielectric function by Adler [2] and Wiser [3], for further discussion see [4–6].

No matter the spectrum being simulated, modelling EEL spectra relies on constructing a model and then running a computer code based on a theoretical treatment of the excitation process. There are three important ingredients:

(a) The model of the system;
(b) The theoretical treatment of the excitation process;
(c) The computational power available.

The review aims to cover:

(a) Improvements / developments in structure prediction techniques, including why it is important and what the effect on our ability to model spectra is.
(b) New theoretical developments: The need for theory to interpret the phonon region of the EELS spectrum and the development of new functionals for density functional theory (DFT) which have the potential to allow us to model a wider range of materials.
(c) Ways of making larger systems more tractable.

1.1. High-resolution EEL spectroscopy

Whilst this review is mainly concerned with EEL spectroscopy carried out within the (S)TEM, it is useful to mention the very closely related technique, reflection, or high-resolution, EEL spectroscopy (HREELS). In HREELS, the beam of electrons (of energy 2–20 eV [20] rather than the 10–100 s of keV energies used for (S)TEM) is reflected from the sample. The technique is used to investigate surfaces, often with molecules absorbed onto them [21], and has been used for looking at phonons [21, 22], plasmons [22] and magnons [23]. Details of the technique can be found in [21, 22]. Recent advances in modelling HREELS data from first principles includes work showing the importance of including both the elastic and inelastic signals [24] and using a quantum-mechanical treatment of the probe electron [25]. In addition, Nazarov has discussed the correct form of the energy loss function for both reflection and transmission EEL spectroscopy for quasi-2D materials and developed an *ab initio* approach for modelling these materials using periodic codes [26].

1.2. Comparison of experimental and simulated data

The comparison of experiment and theory is not necessarily straightforward. It is usually done in a qualitative manor [27] and there is a hierarchy of comparison: Are there the correct number of peaks? Are the peaks in the right places? Are the intensities correct? Some authors have tried a more quantitative method for comparing different approximations and experiment, such as the χ^2 method employed by McCulloch *et al* [27]. Often, however, theory does not reproduce experiment exactly. There are a large variety of reasons for this, for example the level of approximation in the theory being used may not be adequate or the experimental data may contain more than one bonding environment. Often what is more important than reproducing exactly the experimental data is understanding the origin of a difference between spectra or relating a peak to a structural feature. Understanding something about the material or sample is generally the aim of the modelling.

2. Structure prediction

The first step in simulating an EEL spectrum is to construct a model of the sample you are interested in. If the material is well known and well characterised, there are databases of crystal structures, such as the Inorganic Crystallographic Structural Database, ICSD [28, 29], which can provide atomic co-ordinates. Much characterisation, however, is done on materials about which less is known; often that is the motivation behind the research. It then becomes necessary to find an alternative approach to constructing a model. Sometime it is possible to use our chemical knowledge about similar materials to construct viable structures. These can then be compared using DFT to see which structure is most energetically favourable.

In the past decade computational methods have been developed to discover new materials [30, 31]. It is now possible to systematically use existing knowledge and databases in data mining approaches, which rely less on imagination and intuition [32, 33]. In addition, structure prediction from first principles which needs little or no pre-existing knowledge is now also possible [30]. There are several different approaches to first principles structure prediction, including random sampling [34–36], evolutionary algorithms (see references in [30, 37]) and minima hopping [38, 39]. Experimental data can help structure prediction techniques by providing constraints or data to compare with. Structure prediction is not confined to bulk structures, but can be used for interface [40, 41] and defect structure prediction [42–44].

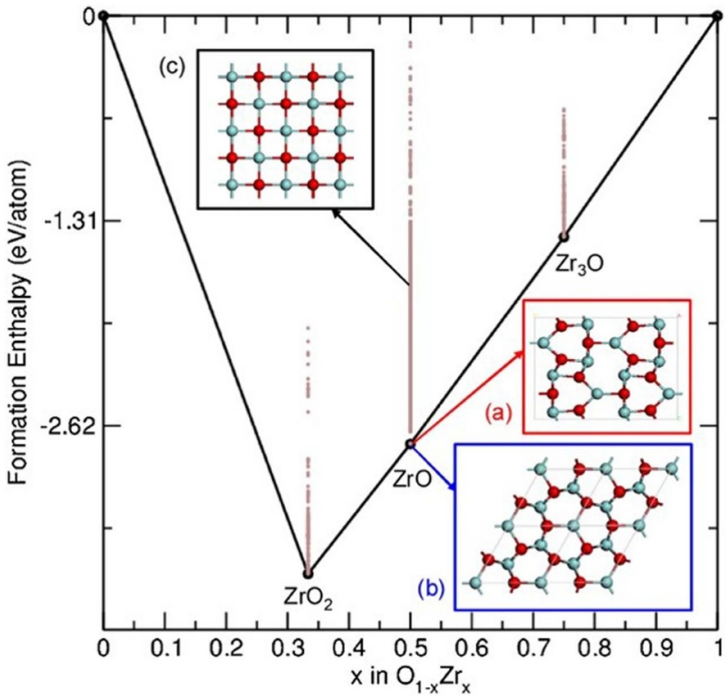

Figure 1. Convex hull of the $O_{(1-x)}Zr_x$ system. The two stable forms of ZrO are shown; the orthorhombic structure (a) has Cmcm symmetry ($a = 3.24$ Å, $b = 12.21$ Å, and $c = 8.59$ Å) and the hexagonal structure (b) has P-62 m symmetry ($a = 5.31$ Å and $c = 3.20$ Å). The experimentally reported cubic rock salt structure (c) is also shown ($a = 4.62$ Å). Oxygen atoms are shown in red. Figure and caption reproduced under the Creative Commons Attribution Licence from Nicholls *et al* Advanced Engineering Materials, 17 (2015) 211.

Structure prediction is becoming more utilised in materials science [45], and with initiatives such as the Materials Project [46, 47], the trend is likely to continue. The Materials Project itself includes an x-ray absorption module which uses FEFF9 [48] to simulate x-ray absorption spectra, which are very similar to EEL spectra. TEM and EEL spectroscopy can provide constraints as well as information to test structure prediction against. Constraints can include, for example, composition or symmetry information. Imaging and spectroscopy can be used to compare model and experimental data as a way of validating a model structure which is important in the case where the structure of a material is unknown [49].

Work combining EEL spectroscopy and an *ab initio* random structure searching (AIRSS) algorithm developed by Pickard and Needs [34, 50] on ZrO show the power of combining structure prediction and electron microscopy [51]. Zirconium based alloys are used for fuel cladding and structural components in water-cooled nuclear reactors. Much effort has gone into optimising these materials to withstand the harsh environment and the lifetime of the zirconium cladding is limited by oxidation caused by water corrosion [52]. The oxidation process had been linked to a sub-oxide phase which forms at the interface between Zr metal and ZrO_2 [53] and, though the composition of the phase had been determined using EEL spectroscopy, the structure was unknown. Low-loss EEL spectra taken across the interface showed distinct signals from the metal, sub-oxide and oxide [51]. To use modelling to understand the structure of the ZrO sub-oxide it was first necessary to produce candidate structures and this was done using AIRSS. For a series of randomly generated structures with the correct stoichiometry, geometry optimisations were carried out using DFT to find a local minima in the energy landscape. All optimised structures were then ranked according to energy to produce a convex hull, as shown in figure 1. One of the most interesting aspects of this work was that the AIRSS produced two structures which could not be distinguished energetically using DFT as the difference in their formation energies was 0.002 eV per formula unit. EEL spectra and diffraction patterns were simulated from the two structures and compared with experiment to determine the structure of the ZrO. Only one of the structures predicted from first principles was able to explain all the experimental data. Both structure prediction and experimental EEL spectra were necessary to determine the structure which is now routinely identified (for example by EBSD [54]) at the grain boundary.

The first important ingredient in modelling EEL spectra is the model of the system. Being able to predict structures from first principles gives us a much wider variety of structures to consider and releases us from the constraints of our own imagination.

3. Developments in theoretical descriptions of the excitation process

EEL spectra span a large energy range and, as mentioned in the introduction, includes different types of energy loss events including phonons, plasmons and core-electron excitations. Although the loss function contains information about all of these different excitations, the different energy ranges and dominating physics often mean that different approaches are taken to model spectra from the different types of excitation.

3.1. Phonon spectroscopy in the transmission electron microscope

Phonons are a materials specific property and phonon dispersions have been probed experimentally using neutrons since the 1950s [55]. The theory of lattice dynamics is well developed [56] and first principles calculations can be used to calculate phonon dispersions [57, 58]. The challenge in interpreting different types of experimental data is knowing which modes contribute to the spectrum, and with what intensity.

Electrons have been used to probe phonons in materials since the 1960s using HREELS [21] (see section 1.1). Recent developments in hardware have allowed phonon vibrations to be seen in the TEM using EEL spectroscopy [59]. Theoretical treatments developed for HREELS are not applicable to transmission EEL spectroscopy due to the geometrical constraints present in reflection EEL spectroscopy. Advances in theory of the excitation of phonons in transmission EEL spectroscopy have allowed first-principles calculations to aid interpretation of the experimental data.

For phonon scattering in transmission EEL spectroscopy, two different regimes have been identified by Dwyer *et al* [60]: dipole scattering and localised vibrational scattering. Dipole scattering involves small momentum transfer and can be carried out in aloof mode, i.e. with the beam next to, but not traversing, the sample. Several approaches to modelling spectra in the dipole regime have been developed [60–64]. In one of the earliest works, Rez [61] looked at the theoretical response of a diatomic molecule and predicted that the signal associated with phonons would be of a similar strength to that from core-loss excitations. Saavedra and García de Abajo [62] have used a Hamiltonian formalism to describe the interaction between the fast (beam) electron and an atomic cluster. They use a classical external potential to describe the electron and a second-quantisation formalism for the phonons. They applied the theory to graphene clusters of varying size and made the link between the spectrum and density of vibrational states.

Radtke *et al* [63] have used a classical approach to relate the EELS spectrum obtained in an aloof geometry to the low-frequency dielectric tensor. By using DFT to calculate the dielectric tensor they were able to interpret data from a guanine crystal, see figure 2. Radtke *et al* [65] have also shown how the symmetry of the phonon modes can be retrieved from orientation dependent aloof beam experiments on anisotropic $B_{12}P_2$ crystals. A semi-classical approach was also used by Hohenester *et al* to calculate the $q = 0$ spectra obtained from MgO nanocubes [64, 66]. A classical response theory has been used by Govyadinov *et al* [67] to show the existence of hyperbolic phonon polaritons in hexagonal boron nitride, which is important for the interpretation of aloof spectra for strongly anisotropic materials.

In terms of the localised vibrational scattering regime, Forbes and Allen [69] have used a transition potential approach and looked at the spatial effect of the beam geometry. Nicholls *et al* have extended the scattering theory for neutrons and x-rays to include electrons used it to interpret momentum resolved measurements from cubic and hexagonal boron nitride [70, 71], see figure 3. A similar approach has been used by Senga *et al* to compare insulating hexagonal boron nitride and its semi-metal carbon counterpart graphite [72]. Hage *et al* [73] have used the phonon density of states to interpret the vibrational signal associated with a single impurity atom in graphene. They show the importance of constructing a large supercell to reduce artificial localisation for defects.

Transmission phonon EEL spectroscopy is an exciting new development in the exploration of lattice dynamics and, to make the most of this new experimental technique, interpretation of spectra using the newly developed theoretical frameworks will be key.

3.2. Advances in DFT functionals

DFT provides the basis of many EEL spectra calculations and the quality of the predicted spectrum is a reflection of the ability of DFT to model a particular material. One of the main approximations in DFT is the treatment of the exchange-correlation term and this is the main limitation in the prediction of ground state structures by DFT [74]. The earliest and simplest treatment of this term was to use the local density approximation (LDA) when the potential is a function of the local density only [75]. The generalised gradient approximation (GGA) also includes information about the gradient of the charge density, but, unlike LDA, there is no single universal form [75]. The Perdew–Burke–Ernzerhof [76] functional is most widely used form of GGA functional and is currently the 'standard' for a DFT calculation.

It is possible to go beyond this and include the second derivative of the electron density in what is known as a meta-GGA functional and many types of meta-GGA have been developed [77]. In addition to the

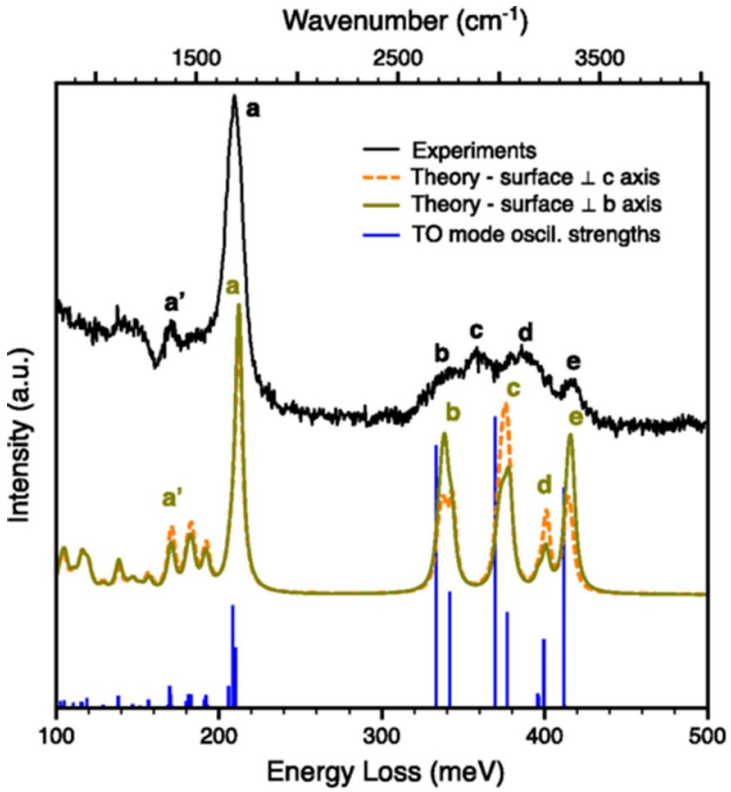

Figure 2. Comparison between the experimental [68] and theoretical vibrational EELS spectra of β-guanine. Two spectra have been calculated, corresponding respectively to a surface perpendicular to the crystal *c* axis and perpendicular to the crystal *b* axis. The 60 keV electron beam is perpendicular to the molecular plane and travels at a distance of $b = 30$ nm from the specimen edge. Blue sticks show the theoretical TO mode oscillator strengths and frequencies. Reprinted figure and caption with permission from G Radtke, D Taverna, M Lazzeri, and E Balan, Phys. Rev. Lett., 119, 027402, 2017. Copyright 2017 by the American Physical Society. http://dx.doi.org/10.1103/PhysRevLett.119.027402.

semi-local functionals, there are also non-local and hybrid functionals (which include an amount of Hartree–Fock exchange energy) and the variety can be daunting. Many of the meta-GGAs have been developed empirically (based on the energies, rather than electron densities) for a specific class of materials. As a result, the functionals are not generally good for a wide variety of materials. Medvedev *et al* [78] have highlighted the dangers of empirical fitting for functionals.

SCAN [79, 80] is a recently developed meta-GGA which includes orbital kinetic energy density terms and satisfies all known constraints for a semi-local functional. Because it has not been fitted to a particular system it can predict diverse types of bonding, including intermediate van der Waals interactions [81]. This is a general functional and so far has been shown to describe materials at least as well as GGA [82, 83]. It has been used for a variety of materials including metal surfaces [84], defects in semiconductors [81], ice [81] and ferroelectrics [85]. It is the first functional to be able to describe cuperate superconductors without any free parameters [86]. This functional has the potential to allow the simulation of a larger variety of systems without the requirement of using system-specific functionals, making them more accessible to modelling of EEL spectra.

4. Approaches to making larger calculations more tractable

EEL spectra simulations can get larger computationally for two main reasons: one is that the number of atoms, i.e. the size of the chunk of material being modelled, increases. This could be due to decreasing core-hole–core-hole interactions, looking at a defect, or simply looking at a material with a large unit cell. The second way calculations can get more computationally intensive is to increase the complexity of the calculation. A standard DFT calculation calculates the ground state of a system. The very nature of doing EEL spectroscopy involves looking energy lost to excitations within the system—the system is no longer in the ground state. Standard DFT calculations of core-loss spectra carried out with a core hole (an electron missing from the core state of the excited atom) are often useful for interpreting spectra [19]. For some materials, it is necessary to use using methods that go beyond standard DFT [6] such as the Bethe-Salpeter

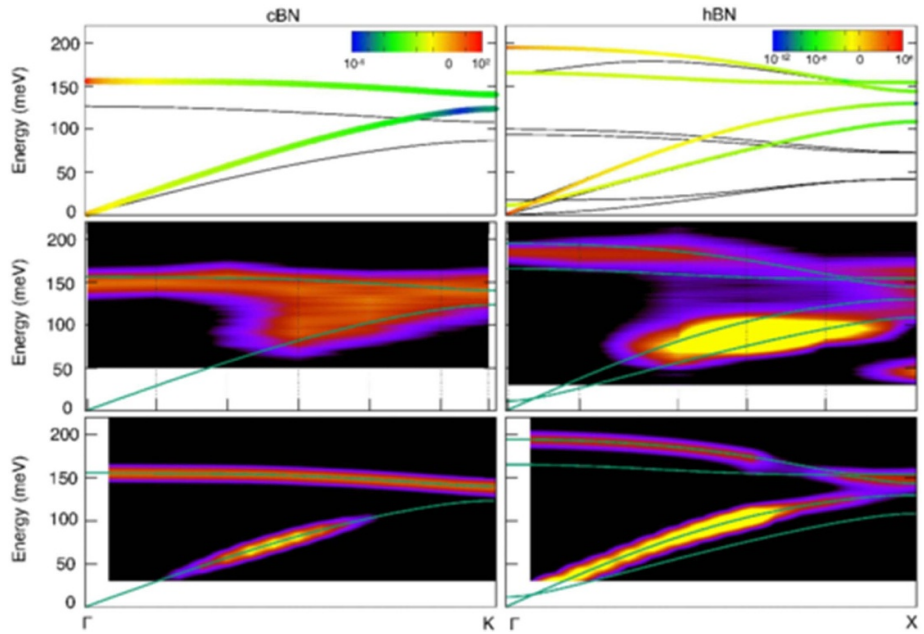

Figure 3. Comparison of experimental and computed dispersion relations for cBN (left) and hBN (right). Upper panel: Calculated phonon dispersion spectra. The bands are coloured according to their intensity on a $\log_{10}$ scale. Inactive bands are shown in black. Middle panel: experimental intensity, normalized by the value of the intensity in the upper branch. The momenta at which the data was recorded is shown by dashed vertical lines and the plot is generated by interpolating between the datapoints. The computed DFT band structure is shown in green. Lower panel: computed intensity, normalized by the value of the intensity in the upper branch. Reprinted figure and caption with permission from R J Nicholls, F S Hage, D G McCulloch, Q M Ramasse, K Refson, and J R Yates, Phys. Rev. B, 99, 094105, 2019. Copyright 2019 by the American Physical Society. http://dx.doi.org/10.1103/PhysRevB.99.094105.

equation, the GW approximation and time-dependent DFT. Many of the implementations of these methods build on a ground state DFT calculation.

Whilst it is possible to conceive and construct ever larger and more complex models and simulations, what can actually be calculated is restricted by the amount of computational power available. Improvements in hardware and software mean that calculations are continually able to become faster and more complex. The increase in the availability of computing power is one of the driving forces behind the development of structure prediction methods discussed above.

As more atoms are included in a DFT calculation, it gets larger in terms of the computational resources it requires. Different approaches have been used to try and decrease the computational expense of calculations. Several authors have developed approaches to combine all electron and pseudopotential methods. In all-electron methods, all the electrons in the atom are included in the calculation, whilst in pseudopotential methods the core electrons (which do not take part in bonding) are replaced with a more slowly-varying pseudopotential. As such, pseudopotentials reduce the computational cost of a simulation. Donval *et al* [87] have developed a hybrid approach for light elements where the corehole effect can be neglected by combining WIEN2k and VASP [88]. They have applied this method to study the silicon $L_{2,3}$ edge. MADNESS is a molecular DFT code [18] which is able to assign atoms as all-electron or pseudopotential within one calculation. It is able to calculate core-edge spectra, including a core-hole [89]. In addition, MADNESS also uses a wavelet basis set, which is computationally efficient [18] and makes it ideal for modelling non-periodic systems.

In general the size of a calculation scales with the cube of the number of atoms. Linear scaling DFT methods have been developed which scale linearly with the number of atoms involved. One such code, ONETEP [16, 17], can calculate up to 3–4000 atoms, and is also able to calculate EEL spectra [90]. Potential applications of such large structures include large supercells to minimise core-hole—core-hole interactions and calculating the spectra of defect atoms, surface atoms or structures such as interfaces and grain boundaries. ONETEP has already been used to investigate anatase surfaces and defects [90] (note: in these examples wavefunction truncation was applied, but kernal truncation was not as the systems were not large enough for it to be advantageous).

Computationally, when using DFT, one of the difficulties with running core-loss calculations is that you are normally interested in the energy range 20–30 eV above the edge onset. The number of states needed to correctly describe this energy range increases as you increase the size of the unit cell leading to a possibly

worse than cubic scaling with number of atoms. Core-loss EELS calculations can still be computationally demanding, i.e. at the limit of what is reasonably possible, and whilst that means that currently some calculations are too big to run, we can look forward to improvements in the future.

5. Conclusions

This review paper has highlighted the potential for impact for several recent advances in first principles simulations of EEL spectra. Advances in structure prediction can open up the field of candidate structures for materials where the structure is not known. Combining structure prediction with EEL simulations can be very powerful and it is likely to be seen more often in the future. Advances in microscope hardware which have allowed phonons to be detected within the TEM have been the catalyst for advances in the theory to describe the spectra obtained. Already we are seeing the importance of having theory to explain the experimental spectra. In addition, the meta-GGA functional SCAN has the potential to allow a wider variety of materials to be studied using the combination of EEL spectroscopy and modelling.

It is still the case that EEL calculations can be computationally demanding. Going beyond DFT is important for a variety of materials, and there are still areas in which there is a lot of opportunity for advancing and improving simulations. Each advance in modelling opens up the variety of problems that can be tackled and the materials and phenomena that can be understood, and that is the driving force behind advancing simulation.

Acknowledgment

R J N gratefully acknowledges financial support from the EPSRC through an EPSRC Fellowship, Grant No. EP/L022907/1.

ORCID iD

Rebecca J Nicholls https://orcid.org/0000-0003-3186-9772

References

[1] Egerton R F 1996 *Electron Energy-loss Spectroscopy in the Electron Microscope* 2nd edn (New York: Plenum)
[2] Adler S L 1962 Quantum theory of the dielectric constant in real solids *Phys. Rev.* **126** 413–20
[3] Wiser N 1963 Dielectric constant with local field effects included *Phys. Rev.* **129** 62–9
[4] Onida G, Reining L and Rubio A 2002 Electronic excitations: density-functional versus many-body green's functions approaches *Rev. Mod. Phys.* **74** 601–59
[5] Sottile F, Bruneval F, Marinopoulos A G, Dash L K, Botti S, Olevano V, Vast N, Rubio A and Reining L 2005 TDDFT from molecules to solids: the role of long-range interactions *Int. J. Quantum Chem.* **102** 684–701
[6] Martin R A, Reining L and Ceperley D M 2016 *Interacting Electrons Theory and Computational Approaches* (Cambridge: Cambridge University Press)
[7] Blaha P, Schwarz K, Tran F, Laskowski R, Madsen G K H and Marks L D 2020 *J. Chem. Phys.* **152** 074101
[8] Available at: http://susi.theochem.tuwien.ac.at/ (Accessed November 2020)
[9] Rehr J J, Kas J J, Prange M P, Sorini A P, Takimoto Y and Vila F D 2009 *Abinitio* theory and calculations of x-ray spectra *C. R. Phys.* **10** 548–59
[10] Available at: http://monalisa.phys.washington.edu/feffproject-feff.html (Accessed November 2020)
[11] Clark S J, Segall M D, Pickard C J, Hasnip P J, Probert M J, Refson K and Payne M C 2005 First principles methods using CASTEP *Z. Kristallogr.* **220** 567–70
[12] Available at: www.castep.org/ (Accessed November 2020)
[13] Available at: http://elk.sourceforge.net/ (Accessed November 2020)
[14] Marini A, Hogan C, Grüning M and Varsano D 2009 yambo: an *ab initio* tool for excited state calculations *Comput. Phys. Commun.* **180** 1392–403
[15] Available at: www.yambo-code.org/about/ (Accessed November 2020)
[16] Skylaris C K, Haynes P D, Mostofi A A and Payne M C 2005 Introducing ONETEP: linear-scaling density functional simulations on parallel computers *J. Chem. Phys.* **122** 084119
[17] Available at: www.onetep.org/ (Accessed November 2020)
[18] Ratcliff L E, Thornton W S, Vázquez Mayagoitia A and Romero N A 2019 Combining pseudopotential and all electron density functional theory for the efficient calculation of core spectra using a multiresolution approach *J. Phys. Chem.* A **123** 4465–74
[19] Keast V 2016 Calculating EELS *Transmission Electron Microscopy: Diffraction, Imaging and Spectroscopy* (Berlin: Springer)
[20] Conrad H and Kordesch M E 2017 High resolution electron energy loss spectroscopy, applications *Encyclopedia of Spectroscopy and Spectrometry* 3rd edn (Oxford: Elsevier) p 47
[21] Ibach H and Mills D L 1982 *Electron Energy Loss Spectroscopy and Surface Vibrations* (New York: Academic)
[22] Ibach H 2006 *Physics of Surfaces and Interfaces* (Berlin: Springer)
[23] Vollmer R, Etzkorn M and Anil Kumar P S, Ibach H and Kirschner J 2003 Spin-Polarized electron energy loss spectroscopy of high energy, large wave vector spin waves in ultrathin fcc Co films on Cu(001) *Phys. Rev. Lett.* **91** 147201
[24] Nazarov V U, Silkin V M and Krasovskii E E 2016 Probing mesoscopic crystals with electrons: one-step simultaneous inelastic and elastic scattering theory *Phys. Rev.* B **96** 235414

[25] Nazarov V U, Silkin V M and Krasovskii E E 2016 Role of the kinematics of probing electrons in electron energy-loss spectroscopy of solid surfaces *Phys. Rev.* B **93** 035403
[26] Nazarov V U 2015 Electronic excitations in quasi-2d crystals: what theoretical quantities are relevant to experiment? *New J. Phys.* **17** 073018
[27] McCulloch D G, Lau D W M, Nicholls R J and Perkins J M 2012 The near edge structure of cubic boron nitride *Micron* **43** 43
[28] Hellenbrandt M 2004 The inorganic crystal structure database (ICSD)—present and future *Crystallogr. Rev.* **10** 17–22
[29] Available at: www.psds.ac.uk/icsd (Accessed November 2020)
[30] Oganov A R, Pickard C J, Zhu Q and Needs R J 2019 Structure prediction drives materials discovery *Nat. Rev. Mater.* **4** 331–48
[31] Schleder G R, Padilha A C M, Mera Acosta C, Costa M and Fazzio A 2019 From DFT to machine learning: recent approaches to materials science—a review *J. Phys. Mater.* **2** 03200
[32] Butler K T, Davies D W, Cartwright H, Isayev O and Walsh A 2018 Machine learning for molecular and materials science *Nature* **559** 547–55
[33] Curtarolo G L W, Hart S, Buongiorno Nardelli M, Mingo N, Sanvito S and Levy O 2013 The high-throughput highway to computational materials design *Nat. Mater.* **12** 191–201
[34] Pickard C J and Needs R J 2011 *Ab initio* random structure searching *J. Phys.: Condens. Matter.* **23** 053201
[35] Freeman C M, Newsam J M, Levinea S M and Catlow C R A 1993 Inorganic crystal structure prediction using simplified potentials and experimental unit cells: application to the polymorphs of titanium dioxide *J. Mater. Chem.* **3** 531–5
[36] Schmidt M U and Englert U 1996 Prediction of crystal structures *J. Chem. Soc. Dalton Trans.* 2077–82
[37] Oganov A R, Lyakhov A O and Valle M 2011 How evolutionary crystal structure prediction works—and why *Acc. Chem. Res.* **44** 227–37
[38] Goedecker S 2004 Minima hopping: an efficient search method for the global minimum of the potential energy surface of complex molecular systems *J. Chem. Phys.* **120** 9911
[39] Amsler M and Goedecker S 2010 Crystal structure prediction using the minima hopping method *J. Chem. Phys.* **133** 224104
[40] Schusteritsch G, Hepplestone S P and Pickard C J 2015 First-principles structure determination of interface materials: the Ni_xInAs nickelides *Phys. Rev.* B **92** 054105
[41] Zhao X, Shu Q, Nguyen M C, Wang Y, Ji M, Xiang H, Ho K-M, Gong X and Wang C-Z 2014 Interface structure prediction from first-principles *J. Phys. Chem.* C **118** 9524–30
[42] Morris A J, Pickard C J and Needs R J 2008 Hydrogen/silicon complexes in silicon from computational searches *Phys. Rev.* B **78** 184102
[43] Morris A J, Pickard C J and Needs R J 2009 Hydrogen/nitrogen/oxygen defect complexes in silicon from computational searches *Phys. Rev.* B **80** 144112
[44] Kaczmarowski A, Yang S, Szlufarska I and Morgan D 2015 Genetic algorithm optimization of defect clusters in crystalline materials *Comput. Mater. Sci.* **98** 234–344
[45] Hermann A and Kurzydłowski D 2019 First-principles prediction of structures and properties in crystals *Crystals* **9** 463
[46] Available at: materialsproject.org/about (Accessed November 2020)
[47] Jain A *et al* 2013 Commentary: the materials project: a materials genome approach to accelerating materials innovation *APL Mater.* **1** 011002
[48] Mathew K, Zheng C, Winston D, Chen C, Dozier A, Rehr J J, Ong S P and Persson K A 2018 High-throughput computational x-ray absorption spectroscopy *Sci. Data* **5** 180151
[49] Wynn J M, Medeiros P V C, Vasylenko A, Sloan J, Quigley D and Morris A J 2017 Phase diagram of germanium telluride encapsulated in carbon nanotubes from first-principles searches *Phys. Rev. Mater.* **1** 073001(R)
[50] Pickard C J and Needs R J 2006 High-pressure phases of silane *Phys. Rev. Lett.* **97** 045504
[51] Nicholls R J, Ni N, Lozano-Perez S, London A, McComb D W, Nellist P D, Grovenor C R M, Pickard C J and Yates J R 2015 Crystal structure of the ZrO phase at zirconium/zirconium oxide interfaces *Adv. Eng. Mater.* **17** 211–15
[52] Nikulina A V 2003 Zirconium-niobium alloys for core elements of pressurized water reactors *Metal Sci. Heat Treat.* **45** 287–92
[53] Ni N, Lozano-Perez S, Sykes J and Grovenor C R M 2011 Quantitative EELS analysis of zirconium alloy metal/oxide interfaces *Ultramicroscopy* **111** 123–30
[54] Hu J, Garner A, Ni N, Gholinia A, Nicholls R J, Lozano-Perez S, Frankel P, Preuss M and Grovenor C R M 2015 Identifying suboxide grains at the metal-oxide interface of a corroded Zr–1.0%Nb alloy using (S)TEM *Trans. EBSD EELS. Micron* **69** 35–42
[55] Brockhouse B N 1995 Slow neutron spectroscopy and the grand atlas of the physical world *Rev. Mod. Phys.* **67** 735
[56] Dove M T 1993 *Introduction to Lattice Dynamics* (Cambridge: Cambridge University Press)
[57] Baroni S and de Gironcoli S, Corso A D and Giannozzi P 2001 Phonons and related crystal properties from density-functional perturbation theory *Rev. Mod. Phys.* **73** 515
[58] Gonze X 1997 First-principles responses of solids to atomic displacements and homogeneous electric fields: implementation of a conjugate-gradient algorithm *Phys. Rev.* B **55** 10337
[59] Krivanek O L *et al* 2014 Vibrational spectroscopy in the electron microscope *Nature* **514** 209–12
[60] Dwyer C, Aoki T, Rez P, Chang S L Y, Lovejoy T C and Krivanek O L 2016 Electron-beam mapping of vibrational modes with nanometer spatial resolution *Phys. Rev. Lett.* **117** 256101
[61] Rez P 2014 Is localized infrared spectroscopy now possible in the electron microscope? *Microsc. Microanal.* **20** 671–766
[62] Saavedra J R M and García de Abajo F J 2015 Phonon excitation by electron beams in nanographenes *Phys. Rev.* B **92** 115449–1–5
[63] Radtke G, Taverna D, Lazzeri M and Balan E 2017 First-principles vibrational electron energy loss spectroscopy of β-Guanine *Phys. Rev. Lett.* **119** 027402–1–5
[64] Hohenester U, Trügler A, Batson P E and Lagos M J 2018 Inelastic vibrational bulk and surface losses of swift electrons in ionic nanostructures *Phys. Rev.* B **97** 165418–1–11
[65] Radtke G, Taverna D, Menguy N, Pandolfi S, Courac A, Le Godec Y, Krivanek O L and Lovejoy T C 2019 Polarization selectivity in vibrational electron-energy-loss spectroscopy *Phys. Rev. Lett.* **123** 256001
[66] Lagos M J, Trügler A, Hohenester U and Batson P E 2017 Mapping vibrational surface and bulk modes in a single nanocube *Nature* **543** 529–32
[67] Govyadinov A *et al* 2017 Probing low-energy hyperbolic polaritons in van der Waals crystals with an electron microscope *Nat. Commun.* **8** 95
[68] Rez P, Aoki T, March K, Gur D, Krivanek O L, Dellby N, Lovejoy T C, Wolf S G and Cohen H 2016 Damage-free vibrational spectroscopy of biological materials in the electron microscope *Nat. Commun.* **7** 10945
[69] Forbes B D and Allen L J 2016 Modelling energy-loss spectra due to phonon excitations *Phys. Rev.* B **94** 014110–1–9

[70] Hage F S, Nicholls R J, Yates J R, MuCulloch D, Lovejoy T C, Delby N, Krivanek O L, Refson K and Ramasse Q M 2018 Nanoscale momentum-resolved vibrational spectroscopy *Sci. Adv.* **4** eaar7495
[71] Nicholls R J, Hage F S, McCulloch D G, Ramasse Q M, Refson K and Yates J R 2019 Theory of momentum-resolved phonon spectroscopy in the electron microscope *Phys. Rev.* B **99** 094105
[72] Senga K, Suenaga R, Barone P, Morishita S, Mauri F and Pichler T 2019 Position and momentum mapping of vibrations in graphene nanostructures *Nature* **573** 247–50
[73] Hage F S, Radtke G, Kepaptsoglou D M, Lazzeri M and Ramasse Q M 2020 Single-atom vibrational spectroscopy in the scanning transmission electron microscope *Science* **367** 1124–7
[74] Cohen A J, Mori-Sánchez P and Yang W 2012 Challenges for density functional theory *Chem. Rev.* **112** 289
[75] Martin R M 2010 *Electronic Structure, Basic Theory and Practical Methods* (Cambridge: Cambridge University Press)
[76] Perdew J P, Burke K and Ernzerhof M 1996 Generalized gradient approximation made simple *Phys. Rev. Lett.* **77** 3865
[77] Hao P, Sun J, Xiao B, Ruzsinszky A, Csonka G I, Tao J, Glindmeyer S and Perdew J P 2013 Performance of meta-gga functionals on general main group thermochemistry, kinetics and noncovalent interactions *J. Chem. Theory Comput.* **9** 355–63
[78] Medvedev M G, Bushmarinov I S, Sun J, Perdew J P and Lyssenko K A 2017 Density functional theory is straying from the path toward the exact functional *Science* **355** 49–52
[79] Sun J, Ruzsinszky A, Perdew J P Constrained S and 2015 Appropriately normed semilocal density functional *Phys. Rev. Lett.* **115** 036402
[80] Bartók A P and Yates J R 2019 Regularized SCAN functional *J. Chem. Phys.* **150** 161101
[81] Sun J *et al* 2016 Accurate first-principles structures and energies of diversely bonded systems from an efficient density functional *Nat. Chem.* **8** 831–6
[82] Borlido P, Aull T, Huran A W, Tran F, Marques M A L and Botti S 2019 Large-scale benchmark of exchange-correlation functionals for the determination of electronic band gaps of solids *J. Chem. Theory Comput.* **15** 5069–79
[83] Isaacs E B and Wolverton C 2018 Performance of the strongly constrained and appropriately normed density functional for solid-state materials *Phys. Rev. Mater.* **2** 063801
[84] Patra A, Bates J E, Sun J and Perdew J P 2017 Properties of real metallic surfaces: effects of density functional semilocality and van der Waals nonlocality *Proc. Natl Acad. Sci.* **114** E9188–96
[85] Paul A, Sun J, Perdew J P and Waghmare U V 2017 Accuracy of first-principles interatomic interactions and predictions of ferroelectric phase transitions in perovskite oxides: energy functional and effective Hamiltonian *Phys. Rev.* B **95** 054111
[86] Furness J W, Zhang Y, Lane C, Buda I G, Barbiellini B, Markiewicz R S, Bansil A and Sun J 2018 An accurate first-principles treatment of doping-dependent electronic structure of high-temperature cuprate superconductors *Commun. Phys.* **1** 11
[87] Donval G, Moreau P, Danet J, Larbi S J-S, Bayle-Guillemaud P and Boucher F 2017 A hybrid method using the widely-used WIEN2k and VASP codes to calculate the complete set of XAS/EELS edges in a hundred-atoms system *Phys. Chem. Chem. Phys.* **19** 1320–7
[88] Available at: www.vasp.at/ (Accessed November 2020)
[89] Pi J M, Stella M, Fernando N K, Lam A L, Regoutz A and Ratclif L E 2020 Predicting core level photoelectron spectra of amino acids using density functional theory *J. Phys. Chem. Lett.* **11** 2256–62
[90] Tait E W, Ratcliff L E, Payne M C, Haynes P D and Hine N D M 2016 Simulation of electron energy loss spectra of nanomaterials with linear-scaling density functional theory *J. Phys.: Condens. Matter.* **28** 195202